A Novel FEM Method for Predicting Thermoacoustic Combustion Instability

G. Campa[*1], S.M. Camporeale[1]
[1]Politecnico di Bari
[*] campa@imedado.poliba.it , DIMeG – Sez. Macchine ed Energetica – Politecnico di Bari – via Re David 200, 70125 Bari, Italy

Abstract
Modern gas turbines suffer of the phenomenon of combustion instability, also known as “humming”. The main origin of the instability is considered to be related to the interaction between acoustic waves and fluctuations of the heat released by the flame. Pressure oscillations may cause many damages of the gas turbine and loss of control of the combustion process. This paper presents a novel numerical method in which the governing equations of the acoustic waves are coupled with a flame heat release model and solved in the frequency domain. The paper shows that a complex eigenvalue problem is obtained that can be solved numerically by implementing the governing equations in COMSOL Multiphysics. This procedure allows one to identify the frequencies at which thermoacoustic instabilities are expected and the growth rate of the pressure oscillations, at the onset of instability, when the hypothesis of linear behaviour of the acoustic waves can be applied. Some test cases and examples of applications are described in the paper.

Key Words:
combustion instability, gas turbine, acoustics, wave propagation, eigenfrequencies, growth rate.

1. Introduction

In modern gas turbines equipped with low NOx emission combustion systems, the phenomenon of acoustically driven combustion instability (known also as "humming") represents a severe risk for the safe operation of the plant, since it causes intense vibrations that may damage the engine. The origin of such phenomenon is not completely understood and, moreover, it is not clear which could be the best techniques suitable for either decreasing the risk of instability or lowering its damaging effects [1-4]. This paper shows a method for predicting the onset of acoustically combustion instabilities in gas turbine combustors. The basic idea is that the governing equations of the acoustic waves can be coupled with a flame heat release model and solved in the frequency domain. This procedure allows one to identify the frequencies at which thermoacoustic instabilities are expected and the growth rate of the pressure oscillations, at the onset of instability, when the hypothesis of linear behaviour of the acoustic waves can be applied. A similar approach has been carried out by Martin et al. [5], even if they used a three-dimensional finite element based in-house acoustic solver called AVSP.
The present method can be applied virtually to any three dimensional geometry, provided the necessary computational resources that are, anyway, much less than those required by Computational Fluid Dynamics (CFD) methods. Furthermore, in comparison with the lumped approach that characterize popular Acoustics Networks, the proposed method allows one for much more flexibility in defining the geometry of the combustion chamber. The paper shows that different types of heat release laws, for instance, heat release concentrated in a flame sheet as well as distributed in a larger domain, can be adopted. Moreover, experimentally or numerically determined flame transfer functions, giving the response of heat release to acoustic velocity fluctuations, can be incorporated in the model.
To establish proof of concept, the method is validated against test cases taken from literature and moreover an application to an annular combustion chamber is proposed.

2. Equations

The problem is solved in the frequency domain using the eigenfrequency “Pressure Acoustics” application mode. Since in gas turbine combustion chamber the flow velocity is generally far below the sound velocity, the flow velocity is negligible, except that in some areas, such as conduits of the burners. These areas, in terms of propagation of pressure

waves, can be treated as separate elements that can be modelled by means of specific transfer function matrices, obtained experimentally or numerically through CFD or aeroacoustics codes. Therefore, the flow velocity is considered negligible in comparison with the sound velocity, within the computational domain. Moreover, the effects of viscous losses and heat conduction will be neglected, and the fluid considered an ideal gas, that means that the ratio of the specific heats is supposed constant. Under such hypotheses, in presence of heat fluctuations, the inhomogeneous wave equation can be obtained:

$$\frac{1}{\bar{c}^2}\frac{\partial^2 p'}{\partial t^2} - \bar{\rho}\nabla\cdot\left(\frac{1}{\bar{\rho}}\nabla p'\right) = \frac{\gamma-1}{\bar{c}^2}\frac{\partial q'}{\partial t} \qquad (1)$$

where q' is fluctuation of the heat input per unit volume, overbar denotes a time average mean value and the prime a perturbation. The term at the RHS of Eq.(1) shows that the rate of non-stationary heat release creates a monopole source of acoustic pressure disturbance. In the eigenvalue analysis as well as in a frequency response analysis, pressure wave can be splitted into a function of position $\hat{p}(\mathbf{x})$ multiplied by a complex exponential that is a function of time

$$p' = \hat{p}(\mathbf{x})\exp(i\omega t), \qquad (2)$$

where ω is complex variable, comprising a real part that gives the frequency of oscillations $f = \mathrm{Re}(\omega)/(2\pi)$, while imaginary part gives the growth rate at which the amplitude of oscillations increases per cycle $g = -\mathrm{Im}(\omega)$. If the growth rate is positive, fluctuations over time will grow exponentially with time. Within the harmonic analysis, heat release fluctuation q' and acoustic velocity u' are also functions of time of the type $q' = \hat{q}\exp(i\omega t)$ and $u' = \hat{u}(\mathbf{x})\exp(i\omega t)$. Then, using Eq.(1) and Eq.(2), the acoustic pressure waves are governed by the following equation

$$\frac{\lambda^2}{\bar{c}^2}\hat{p} - \bar{\rho}\nabla\cdot\left(\frac{1}{\bar{\rho}}\nabla\hat{p}\right) = -\frac{\gamma-1}{\bar{c}^2}\lambda\hat{q} \qquad (3)$$

where $\lambda = -i\omega$ and c is the velocity of the sound. Eq.(3) shows a quadratic eigenvalue problem that can be solved by means of an iterative linearization procedure [8].
The finite element method allows us to model the heat release fluctuation q' as a variable of space, so that it is possible to describe the form of the flame in a very flexible manner. In this work, however, the flame is modelled as a straight flame sheet placed at the exit of the burner, in order to accomplish the aim of comparing the numerical results with those of the cited cases available in literature.
The boundary conditions are considered basically as three types: sound hard (wall), sound soft and normal acceleration. The solid walls are considered as sound hard, while the plenum inlet and the combustion chamber outlet walls changes with the different test cases analyzed.

3. Tests on Linear Combustion Chamber

The preliminary application tests are carried out on a duct, with uniform cross-sectional area, mean temperature, constant density and no mean flow. Such a scheme is the same examined by Dowling and Stow in [6] and was chosen as a benchmark. The duct is connected to a large plenum at the inlet and is provided of a restriction at the exit (Figure 1). In this one-dimensional case, the planar wave hypothesis can be adopted and the only abscissa x along the duct is used to describe the variation of acoustic pressure and velocity in the duct. A planar flame sheet is supposed to be located at the abscissa $x=b$. Under the no flow hypothesis, the following boundary conditions are assumed

$$p'(0) = 0,\ u'(l) = 0. \qquad (4)$$

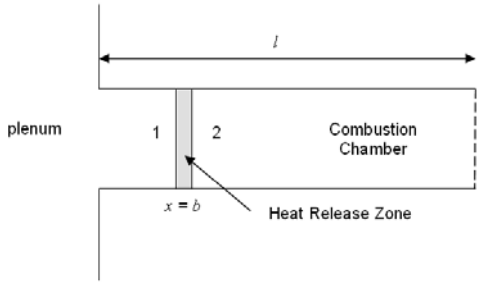

Figure 1 – Simplified scheme of flame location in a straight duct with uniform cross section.

Dowling and Stow offer an example where the heat release fluctuation is supposed to be concentrated in a single plane placed at $x=b$ (Figure 1) and related to the velocity fluctuation of the oncoming flow with a time delay τ

$$q'(x,t) = Q'(t)\delta(x-b) \qquad (5)$$

$$Q'(t) = -[\beta \bar{\rho} \bar{c}^2/(\gamma-1)]\; u'_1(t-\tau) \qquad (6)$$

where $Q'(t)$ is the rate of heat input per unit area of the cross section of the duct and subscript 1 denotes conditions just upstream of this region of heat input, that is $u'_1(t) = u'(b^-,t)$. The Eq.(5) relates the fluctuation of heat input rate per unit volume, $q'(x,t)$, to the fluctuation of the heat input rate per unit area of the cross section, $Q'(t)$, through the Dirac's delta $\delta(x-b)$. The nondimensional number β gives a measure of the intensity of the heat fluctuations while τ can be estimated as the convection time from fuel injection to its combustion.

In the FEM eigenvalue analysis, the heat release fluctuations are supposed to occur in a very thin volume with thickness s and the Dirac's delta $\delta(x-b)$ that appears in Eq.(9) can be approximated as:

$$\delta(x-b) \cong \begin{cases} 0 & x \le b - s/2 \\ 1/s & b - s/2 < x \le b + s/2 \\ 0 & x > b + s/2 \end{cases}. \qquad (7)$$

Using Eq.(2), setting $\lambda = -i\omega$ and simplifying, Eq.(3) becomes

$$\frac{1}{\bar{\rho}}\frac{1}{\bar{c}^2}\left(\lambda^2\right)\hat{p} - \frac{1}{\bar{\rho}}\nabla(\nabla\hat{p}) = \left[-\beta\delta(x-b)(-\lambda)\hat{u}(b^-)\exp(-\lambda\tau)\right] \qquad (8)$$

that is the governing equation to be solved in the internal domain by the FEM method.

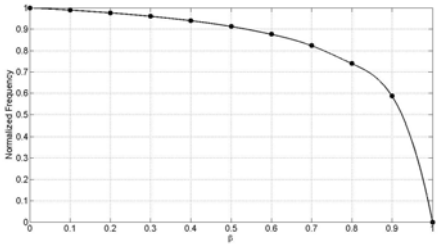

Figure 2 – Variation with β of the normalized frequency for the first mode of the duct with heat release fluctuation concentrated in a flame sheet. Time delay τ=0 and b=l /10. Symbols represent the results from the acoustic code. Line is obtained from the analytic solution.

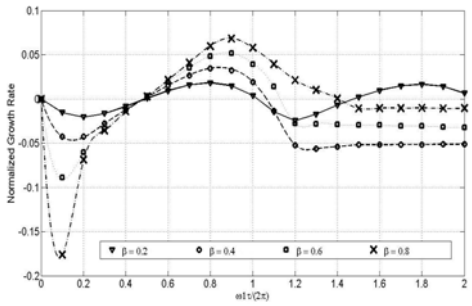

Figure 3 – Variation with β of the growth rate for the first mode of the duct with heat release fluctuation concentrated in a flame sheet. Case b=l/10. Symbols represent the results from the acoustic code. Lines are obtained from the analytic solution.

Figure 2 and Figure 3 show the comparison of the results obtained from the acoustic code and the results obtained from the application of the planar wave theory. It appears a very good agreement for the frequency as well as for the growth rate. The numerical results obtained here appear to be much better than those obtained from the one-term Galerkin approximation given in [6]. The dependence of the resonant frequency on β is shown in Figure 2. As β increases, the intensity of the heat release in the combustion chamber and the acoustic pressure increase. Consequently, there is a decrease of the resonant frequency in a measure to comply with inlet and outlet boundary conditions. The influence of β and τ on the growth rate is shown in Figure 3. Growth rate increases if the rate of heat input has a component in phase with pressure perturbation. The differences between the results obtained from the FEM analysis are so close to those obtained analytically that graphically any difference can be observed, confirming the success of this test.

In the previous examples, only a theoretical geometry has been considered, suitable for benchmark tests, since the analytical solutions exist for such tests. In [6] Dowling and Stow examine a more realistic quasi-one-dimensional geometry, composed by three cylindrical ducts: diffuser, premixer and combustion chamber. In this case, a low Mach number flow was considered in [6], while here the flow is neglected according with Eq.(1). It is assumed, following the approach adopted in [6], the blockage at the premixer inlet so that it acts approximately like a hard end (u'=0). An open end is instead assumed at the combustor exit (p'=0).

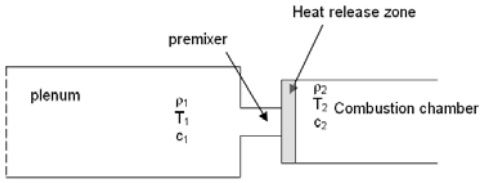

Figure 4 - Simplified scheme of flame location and boundary conditions, for benchmark tests on straight duct with variation of section.

The flame sheet is supposed to be placed at the exit of the premixer, just at the inlet of the combustion chamber. The heat release fluctuation, given by Eq.(6), is related to the fluctuations of the flow velocity at the fuel inlet point through a time delay τ. The flame model used by Dowling and Stow in [6] was

$$\frac{\hat{Q}}{\overline{Q}} = -k\frac{\hat{m}_i}{\overline{m}_i}\exp(-i\omega\tau) \qquad (9)$$

where m_i is the air mass flow at the fuel injection point (assumed to be located at the inlet of the premixer). k is a nondimensional number, used for varying the intensity of the unsteady heat release. The time average of heat release rate per unit area of the combustion chamber is

$$\overline{Q} = \rho_i \overline{u}_i c_p \left(\overline{T}_2 - \overline{T}_1\right)\frac{A_{\text{premix}}}{A_{\text{comb.chamb.}}} \qquad (10)$$

where c_p is specific heat at constant pressure and $\overline{T}_1$ and $\overline{T}_2$ are the temperatures in the premixer and in the combustion chamber, respectively. From these equations, an expression of $\hat{Q}$ can be obtained. Then the heat input per unit area can be written as a function of time $Q' = \hat{Q}\exp(i\omega t)$. So that, by using Eq.(5), it is straightforward to obtain the expression of the coefficient β to be used to quantify the fluctuations of heat release in Eq.(8) where, coherently with the flame model assumed here, the velocity fluctuation at the premixer inlet, $\hat{u}_i$ has been considered instead of the fluctuation $\hat{u}(b^-)$ just upstream of the flame.

The grid used for this case, composed of 11382 elements uniformly distributed, is represented in Figure 5:

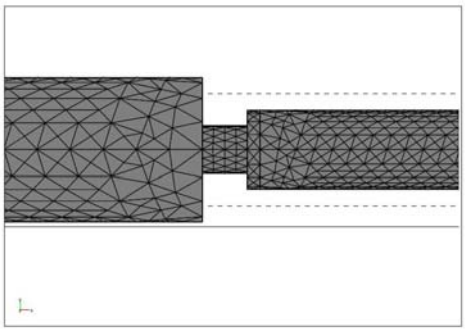

Figure 5 – Mesh visualization of the quasi-one-dimensional combustion system

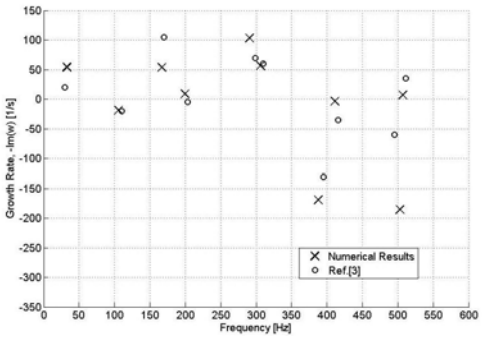

Figure 6 – Resonant mode of a simple combustor. Crosses represent the results from the acoustic code. Circles represent the results from [6]

The results obtained from the calculations of the eigenvalues of the system with heat release fluctuations with k=1 are given in Figure 6, where the values of growth rate values are plotted against the frequency values. In this figure such results are compared with the corresponding values given in [6]. It appears that the code is able to identify the all the modes and their frequencies, carefully. Also the growth rate is well estimated taking into account that calculations in [6] are carried out under the hypothesis of planar waves and taking into account the damping effects due to the mean flow. In many cases heat release fluctuations have the effect to create instability as the growth rate has a positive value. The analysis of the pressure patterns of each mode, show that the lowest frequency of 29 Hz corresponds to a resonance of the whole system, 105 [Hz] is the frequency of the first mode of the plenum, that behaves like an acoustic tube with a closed end at the inlet and an approximately closed end at the other boundary due to the variations of the cross section at the conjunction with the premixer. Further eigenfrequencies appear at 199, 290, 387 and 502 Hz that are the harmonics of the mode at 105 Hz. A good correspondence with

the results shown in [6] is obtained. In fact all the important frequencies are valuated. The growth rate are not equal because mean flow is neglected, following a conservative analysis. In this way growth rate are greater in absolute value than those obtained in [6] and tightened to instability.

4. Tests on Annular Combustor

The examination of an annular combustor has been carried out taking as reference the simple geometry examined by Pankiewitz and Sattelmayer in [7]. The combustor, shown in Figure 7, is characterized by a diffusion chamber ring (plenum) and an annular combustion chamber linked by 12 "swirler" burners. The hot gases leave the combustion chamber through 12 choked nozzles, which allow the achievement of high pressure inside the chamber. The conditions are set according to a case of an experimental combustor that was operated with natural gas, the air entering the plenum being preheated to T_1 = 770K and the total thermal power being P = 1020kW. In Figure 7 the grid composed of 66519 elements uniformly distributed is represented.

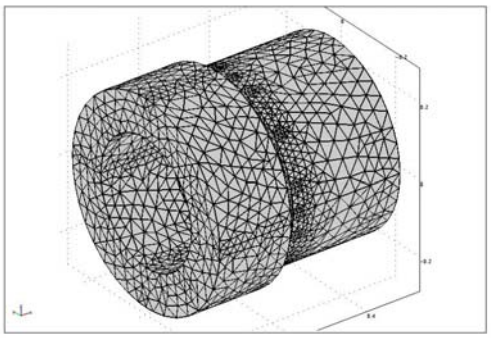

Figure 7 – Computational grid of the annular combustion chamber.

For inlet and outlet boundary conditions the same approach used in [7] is adopted in order to take into account the effects of the flow velocity on acoustic impedance of such boundaries. The flow both enters and exits the computational domain from and to a large plenum, where pressure perturbations can be neglected. Defining the inward normal acceleration at the boundary as

$$a'_n = -\mathbf{n} \bullet \frac{\partial \mathbf{u}'}{\partial t}, \qquad (11)$$

taking into account the equation $\frac{\partial \mathbf{u}'}{\partial t} + \frac{1}{\overline{\rho}} \nabla p' = 0$ and considering that $p' = \hat{p} \exp(i\omega t)$, the expression of normal acceleration can be written as

$$\hat{a}_n = -i\omega \frac{1}{\overline{\rho}} \cdot \frac{K}{K\overline{u}_n + \frac{1}{\overline{\rho}}} \hat{p} \qquad (12)$$

where, like other fluctuating quantities, $\hat{a}_n$ is obtained from the relation $a'_n = \hat{a}_n \exp(i\omega t)$. Assuming a suitable value for the constant $K = \overline{u}_n / 2(\overline{p} - p_\infty)$, Eq.(12) gives the expression of normal acceleration that is used in COMSOL to set the boundary conditions at inlet and outlet of the combustion system [8]. The value K = 0 represents the condition of choked or closed end; $K = \infty$ represents the condition of open end. As in [7], the values of K = 0.1 at inlet and K = 0.2 at outlet, are assumed in the calculations.

The eigenvalue analysis of the system has been carried out in order to obtain the characteristic modes of the system. At the beginning the system is considered without heat release. The eigenfrequencies have been normalized with the frequency $f_0 = u_0 / L_0$ where u_0 is equal to the sound speed in the plenum and the length L_0 is equal to the mean diameter of the chamber. The obtained results for the first four modes are given in Table 1 and compared with the results given in [7]. The modes are denoted with the nomenclature *(l,m,n)*, where *l*, *m* and *n* are, respectively, the orders of the pure axial, circumferential and radial modes that appear in the eigenmode obtained from simulation. In a distribution of pressure within the whole combustion assembly, for the first four eigenmodes, is presented: pressure distributions appear to be very similar to those proposed in [7]. The first mode is a pure axial mode, the second one is a circumferential mode that involves only the plenum where the largest pressure oscillations can be seen. The third mode is a coupled axial-circumferential mode where the largest oscillations occur in the combustion chamber. The fourth mode is a circumferential mode of the second order that involves only the plenum. The main difference between the results obtained here and those given in [7] appears to be related to the value of the eigenvalue corresponding to the axial mode. This is most probably due to some geometrical differences in the axial length of

some parts in respect to those used in [7] where not all the geometrical details are available. For the circumferential modes, further eigenfunctions can be obtained by rotation around the combustor axis of an angle of $\pi/(2m)$. For the sake of simplicity, only one eigenmode is represented for each frequency.

Table 1 – Values of the normalized frequencies from the acoustic code and from [7].

Mode shape	(1,0,0)	(0,1,0)	(1,1,0)	(0,2,0)
Numerical results	0.243	0.350	0.576	0.658
Ref. [7]	0.390	0.353	0.656	0.668

Mode shape	(1,0,0)	(0,1,0)	(1,1,0)	(0,2,0)
Numerical results	0.243	0.350	0.576	0.658
Ref. [6]	0.390	0.353	0.656	0.668

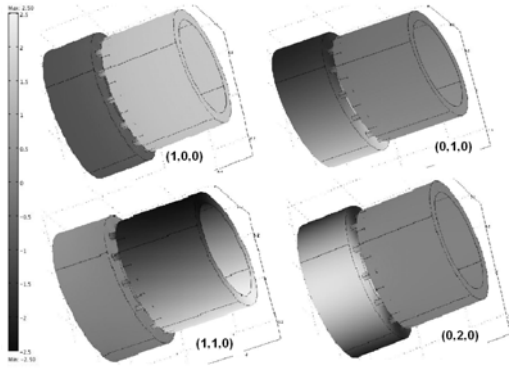

Figure 8 – First four acoustic eigenmodes of the combustor.

Then the system is analyzed considering the presence of heat release. To this purpose the approach proposed in [7] has been followed, adopting the flame model of Eq.(9), that relates the heat release fluctuations to the acoustic velocity at the premixer inlet, as a consequence of the fuel-air ratio fluctuations at the point of fuel input. For each sector of the flame zone, the heat release fluctuation $\hat{Q}$ is related to the acoustic velocities taken upstream of the corresponding burner; the heat release is supposed to be distributed uniformly in each sector of the flame zone. It is worth noting that in [7], the flame response was related to the acoustic velocity at the inlet of the chamber (corresponding to the premixer exit) while, here, the flame model of Eq.(9) relates the heat release fluctuations to the acoustic velocity at the premixer inlet. The eigenvalue analysis of the system has been carried out by varying the values of the parameter k (0.5 to 1) and of the time delay τ (from 0 to 0.006 s).

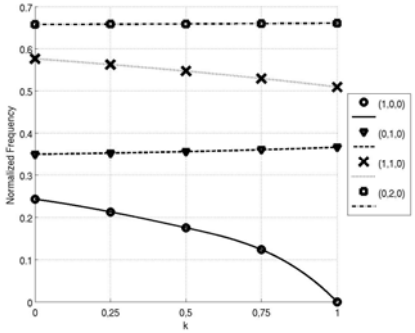

Figure 9 – Variation with k of the normalized frequencies of the annular combustion chamber. Time delay $\tau = 0$.

First of all, the variation of the value of the first four eigenvalues with the parameter k are examined, assuming $\tau = 0$. The results given in Figure 9 show that the frequency of axial mode is strongly influenced by the variation of k: its non-dimensional value decreases from 0.243 with k=0 to zero where k=1. With further higher values of k the axial mode disappears, likewise what is shown previously in Figure 2 for the first mode of the duct with heat release fluctuation. The increase of k produces the increase of the heat release fluctuations in the combustion chamber, the increase of the acoustic pressure therein, and, consequently, the decrease of the eigenfrequency in order to meet the inlet and outlet boundary conditions. The increase of k has instead lower influence on both the frequencies of the circumferential modes in the plenum, while a significant variation of the frequency is observed for the circumferential mode in the combustion chamber.

The second mode is the first circumferential in the plenum (0,1,0). In this case, the highest pressure amplitude occur in the plenum. Such pressure fluctuations are driven by the heat fluctuations in the chamber, notwithstanding that in the chamber the pressure oscillations are much lower. The normalized frequency and growth rate of this mode are shown in Figure 10 where symbols represent the results obtained from simulation and splines connecting the symbols are used in order to give the pattern of the curves. An alternation of stability and instability conditions is observed with the variation of the time delay, and also the increase of k causes the variation the value of the growth rate.

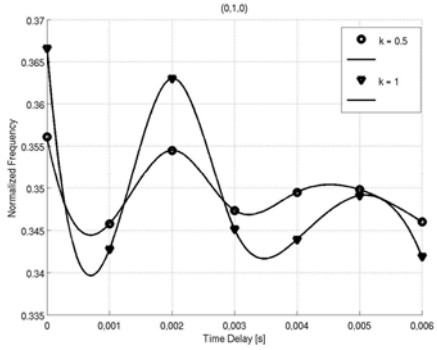

(a)

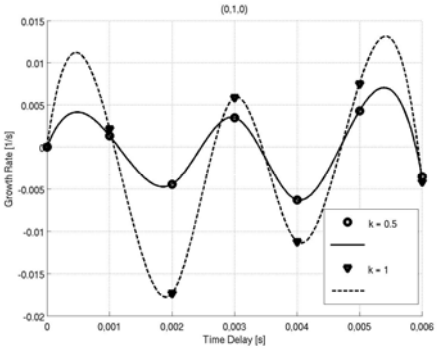

(b)

Figure 10 - Variation with the time delay of the normalized frequency (a) and of the growth rate (b) of the first circumferential mode of the plenum.

5. Conclusion

The present approach is particularly appropriate to treat complex geometries that are difficult to be examined either with analytical methods or acoustic network methods. The FEM analysis has been successfully applied also to different kinds of heat release laws and different boundary conditions. Both stable and unstable eigenmodes have been identified over a wide range of frequencies for different configurations. Frequencies and growth rates are accurately captured, and results are in a very good agreement with results obtained analytically and over simple geometries.

The proposed method appears to be a relatively simple tool for the analysis of combustion instability problems under the simplified hypothesis of linear acoustic waves. The method can be applied, e.g., to the analysis of the effects of passive damping devices or of the effects of the geometry of the system on the combustion stability, after knowing from experiments or CFD analyses, suitable flame response functions and the transfer function matrixes of the burner.

6. References

1. Polifke W.: Combustion Instabilities, Advances in Aeroacoustics and Applications, March 2004.
2. Morse, P. “Vibration and Sound.” American Institute of Physics for the Acoustical Society of America, second edition, 1981.
3. Hathout, J. P.: “Thermoacoustic Instabilities”. *Fundamentals and modeling in combustion*, April 1999.
4. Lieuwen, T., “Modeling Premixed Combustion–Acoustic Wave Interations: A Review,” *Journal of Propulsion and Power*, Vol. 19, No. 5, 2003, pp. 765–781.
5. Martin and Benoit et al., “Analysis of acoustic energy and modes in a turbulent swirled combustor”, Center for Turbulence Research Proceedings of the Summer Program, 2004.
6. Dowling, A.P., and Stow, S. R.: Acoustic Analysis of Gas Turbine Combustors, *Journal of Propulsion and Power*, Vol. 19, No. 5, pp. 751-765, October 2003.
7. Pankiewitz C., Sattelmayer, T., “Time Domain Simulation of Combustion Instabilities in Annular Combustors”, *ASME paper* GT-2002-30063.
8. *COMSOL Multiphysics User’s Manual*, 2007.